OXFORD

Cerebral Cortex, 2023, **33**, 3181–3192
https://doi.org/10.1093/cercor/bhac268
Advance access publication date 19 July 2022
Original Article

Convergent and divergent oscillatory aberrations during visuospatial processing in HIV-related cognitive impairment and Alzheimer's disease

Chloe E. Meehan[1,2], Christine M. Embury[1], Alex I. Wiesman[3], Mikki Schantell[1,4], Sara L. Wolfson[5], Jennifer O'Neill[6], Susan Swindells[6], Craig M. Johnson[7], Pamela E. May[8], Daniel L. Murman[8,9], Tony W. Wilson[1,2,4,10,*]

[1]Institute for Human Neuroscience, Boys Town National Research Hospital, Boys Town, NE 68010, USA,
[2]Department of Psychology, University of Nebraska – Omaha, Omaha, NE 68182, USA,
[3]Montreal Neurological Institute, McGill University, Montreal, QC H3A 2B4, Canada,
[4]College of Medicine, University of Nebraska Medical Center, Omaha, NE 68198, USA,
[5]Geriatrics Medicine Clinic, University of Nebraska Medical Center, Omaha, NE 68198, USA,
[6]Department of Internal Medicine, Division of Infectious Diseases, University of Nebraska Medical Center, Omaha, NE 68198, USA,
[7]Department of Radiology, University of Nebraska Medical Center, Omaha, NE 68198, USA,
[8]Department of Neurological Sciences, University of Nebraska Medical Center, Omaha, NE 68198, USA,
[9]Memory Disorders & Behavioral Neurology Program, University of Nebraska Medical Center, Omaha, NE 68198, USA,
[10]Department of Pharmacology & Neuroscience, Creighton University, Omaha, NE 68178, USA
*Corresponding author: Institute for Human Neuroscience, Boys Town National Research Hospital, 14090 Mother Teresa Ln., Boys Town, NE 68010, USA.
Email: tony.wilson@boystown.org

Adults with HIV frequently develop a form of mild cognitive impairment known as HIV-associated neurocognitive disorder (HAND), but presumably cognitive decline in older persons with HIV could also be attributable to Alzheimer's disease (AD). However, distinguishing these two conditions in individual patients is exceedingly difficult, as the distinct neural and neuropsychological features are poorly understood and most studies to date have only investigated HAND or AD spectrum (ADS) disorders in isolation. The current study examined the neural dynamics underlying visuospatial processing using magnetoencephalography (MEG) in 31 biomarker-confirmed patients on the ADS, 26 older participants who met criteria for HAND, and 31 older cognitively normal controls. MEG data were examined in the time–frequency domain, and a data-driven approach was utilized to identify the neural dynamics underlying visuospatial processing. Both clinical groups (ADS/HAND) were significantly less accurate than controls on the task and exhibited stronger prefrontal theta oscillations compared to controls. Regarding disease-specific alterations, those with HAND exhibited stronger alpha oscillations than those on the ADS in frontoparietal and temporal cortices. These results indicate both common and unique neurophysiological alterations among those with ADS disorders and HAND in regions serving visuospatial processing and suggest the underlying neuropathological features are at least partially distinct.

Key words: neuroHIV; magnetoencephalography; MEG; oscillations.

Introduction

The widespread use of combination antiretroviral therapies (cARTs) has greatly extended life expectancy in people with HIV (PWH) and made HIV a manageable, chronic condition. However, despite such advances in modern medicine, PWH remain at risk for developing neurological comorbidities such as HIV-associated neurocognitive disorder (HAND), which is highly prevalent and affects approximately 50% of the HIV-infected population (Robertson et al. 2007; Namagga et al. 2019). HAND can emerge at any age in PWH and is not uncommon in those in their third and fourth decades of life. In such cases, the likelihood that the cognitive decline is HIV related is generally high, as the incidence of other neurological conditions associated with cognitive impairment within this age range is low. However, conditions like Alzheimer's disease (AD) become much more common later in life and thus, the degree of certainty that cognitive impairments are HIV related becomes much lower in those who first present in their fifth and sixth decades of life (Milanini and Valcour 2017).

Dissociating cognitive impairment due to HAND or an AD spectrum (ADS) condition is challenging given the overlap in affected neurocognitive domains, including deficits in working memory, attention, and visuospatial processing (Woods et al. 2009; Milanini and Valcour 2017; Rubin et al. 2019). Combining cognitive testing with amyloid imaging using positron-emission tomography (PET) is the gold-standard for diagnosing AD, and recent PET studies in PWH have found normal beta-amyloid deposition relative to healthy demographically matched adults, regardless of cognitive status (Fulop et al. 2019; Howdle et al. 2020; Mohamed et al. 2020). Such data provide initial support that the conditions are pathologically distinct,

Received: March 18, 2022. **Revised:** May 24, 2022. **Accepted:** June 12, 2022

although the sample sizes in these studies were relatively modest and both empirical studies remarked that some PWH did exhibit higher amyloid deposition. In the context of HIV, cognitive impairment is generally assumed to be HAND with little consideration of ADS as a possible differential diagnosis, although there are reports of ADS diagnoses in older cognitively impaired PWH (Turner et al. 2016; Calcagno et al. 2021). Thus, neural markers capable of distinguishing cognitive decline due to HIV versus AD pathologies would be of major value and fill a current void that will impact the field's future ability to test new therapeutics targeting the specific pathological features of each condition.

Beyond amyloid PET, numerous studies using structural MRI in groups with either HAND or ADS have identified declines in cortical volume and thickness that are particularly evident within the posterior cortices (Aylward et al. 1995; Lane et al. 2018). Likewise, studies using functional MRI (fMRI) have reported decreases in activation within the dorsal pathway during visuospatial and attentional processing in patients with ADS relative to healthy controls (Prvulovic et al. 2002; Vannini et al. 2008; Thiyagesh et al. 2009), while similar studies in those with HAND have shown abnormal increases in neural activation in the parietal, prefrontal, and occipital cortices (Chang et al. 2001, 2004). Thus, fMRI studies have provided some evidence that the underlying aberrations may differ in those with ADS and HAND, but to date studies comparing the two populations directly are extremely rare.

This abundance of studies in each disease, but lack of direct comparisons, extends to work using magnetoencephalography (MEG). Such MEG studies often make use of the method's excellent temporal and spatial precision, which enables multi-spectral oscillatory activity in the theta (4–8 Hz), alpha (8–14 Hz), beta (15–30 Hz), and gamma (30 + Hz) ranges to be directly quantified. These oscillations are known to serve critical roles in visuospatial processing and attention in healthy adults (Başar et al. 2001; Buzsáki and Wang 2012; van Diepen et al. 2016; Harris et al. 2017). While there are many resting-state studies of patients on the ADS and those with HAND, task-based MEG studies are far less common and thus disease-specific alterations in the neural dynamics serving cognition remain poorly understood. MEG studies of visuospatial processing have shown distinct neural signatures of alpha and gamma activity, with some markers distinguishing cognitively impaired (i.e. HAND) and unimpaired PWH and both groups from controls (Wiesman et al. 2018b). Other MEG work has shown altered age-related trajectories of gamma oscillatory activity in key areas of parieto-occipital and frontoparietal networks in cognitively impaired versus unimpaired PWH and controls (Groff et al. 2020). In patients with ADS, one recent MEG study focusing on visuospatial processing revealed blunted theta and alpha occipital neural responses in those on the ADS relative to cognitively normal controls, with alpha further predicting cognitive status in patients (Wiesman et al. 2021b). However, again, no such studies have directly investigated the extent to which these functional aberrations are shared versus unique in participants with HAND or ADS.

In the current study, we used MEG to probe the neural dynamics supporting visuospatial processing in participants with HAND and those on the ADS. Visuospatial processing is known to be critically affected in those with HAND (Woods et al. 2009) and to rely on the same parietal brain regions that exhibit high amyloid deposition in those on the ADS. Thus, all participants performed a well-established visuospatial discrimination task during MEG recording, which has been shown to elicit multi-band oscillatory activity in parieto-occipital regions, including responses in the theta, alpha, and gamma ranges (Wiesman et al. 2017). Given the previous independent literatures on ADS and HAND pathologies, we hypothesized that those in the ADS group would exhibit weaker neural responses than those in the HAND group and that such differences would be strongest in the alpha range. More broadly, we predicted that these differences would be primarily within parieto-occipital and prefrontal cortices, which are strongly engaged during such visuospatial processing tasks.

Materials and methods

Participants

Thirty-one amyloid-positive patients on the ADS with amnestic mild cognitive impairment (aMCI) or mild probable AD, as determined by a fellowship-trained neurologist specializing in memory disorders, were enrolled in this study. All 31 participants underwent beta-amyloid PET and were deemed biomarker positive. The HAND group consisted of 26 cognitively impaired older PWH who met the Frascati criteria (Antinori et al. 2007) for HAND and were receiving effective cART with undetectable viremia. Participants on the ADS were selected from those enrolled in a larger project examining neurological alterations associated with aging (R01-MH116782-S1), while those with HAND were selected from a larger-scale study of aging with HIV (MH103220) based on their demographics. Finally, a control group of 31 older adults with normal cognition were also enrolled pulling from the control group of each study. Participants were between the ages of 51 and 79. The groups were matched on key demographics except age (i.e. the HAND group was slightly younger than healthy controls and ADS patients). Thus, age was included as a nuisance covariate in all statistical modeling. Exclusion criteria included any medical illness affecting CNS function (other than HIV infection), any neurological disorder (other than AD/aMCI/HAND), history of head trauma, and current substance abuse. The Institutional Review Board at the University of Nebraska Medical Center reviewed and approved these investigations. Written informed consent was obtained from each participant and, where necessary, from a

legally authorized representative as well following detailed description of the study.

Neuropsychological testing

All participants underwent a battery of neuropsychological assessments, with raw scores for each participant being converted to demographically adjusted z-scores using published normative data (Benedict et al. 1998; Brandt and Benedict 2001; Heaton et al. 2004). This battery, which was developed in collaboration with a clinical neuropsychologist specializing in cognitive disorders, assessed multiple functional domains known to be impaired in patients with HAND and those on the ADS. Specifically, the cohort of PWH were assessed on the following cognitive domains per the Frascati criteria (Antinori et al. 2007): *learning*, *memory*, *attention and executive function*, *motor,* and *processing speed*. The AD cohort completed a neuropsychological assessment that assessed commonly impaired cognitive domains in AD: *learning, memory*, *attention and executive function*, *language*, and *processing speed*. In addition, we measured *premorbid function* and *functional impairment* in all participants, along with *general cognitive status* in the AD group. Controls completed one of these two batteries depending on which project they were drawn from. Using these assessments and activities of daily living (ADL), PWH were diagnosed with HAND according to the Frascati guidelines, including subgroups with asymptomatic neurocognitive impairment (ANI; i.e. having at least two cognitive domains one SD below the standardized mean, with no ADL deficits), mild neurocognitive disorder (MND; i.e. at least two cognitive domains one SD below the standardized mean, with ADL deficits), or HIV-associated dementia (HAD; i.e. having at least two cognitive domains two SDs below the standardized mean, with ADL deficits). Healthy controls were cognitively normal and did not meet the above criteria for neuropsychological impairment. For patients on the ADS, instrumental activities of daily living (IADLs) were measured (with an informant) using the Functional Activities Questionnaire (FAQ; Pfeffer et al. 1982). In addition to the neuropsychological battery, general cognitive status was measured using the Montreal Cognitive Assessment (MoCA; Nasreddine et al. 2005) and the Mini-Mental State Examination (MMSE; Folstein et al. 1975).

Florbetapir ^{18}F positron emission tomography

Combined PET/CT data using ^{18}F-florbetapir (Amyvid™, Eli Lilly) and a GE Discovery MI digital scanner (Waukesha, WI) were collected following the standard procedures described by the Society of Nuclear Medicine and Molecular Imaging (3D acquisition; single intravenous slow-bolus < 10 mL; dose = 370 MBq; waiting period = 30–50 min; acquisition = 10 min; Minoshima et al. 2016). Images were attenuation corrected using the CT data, reconstructed in MIMNeuro (slice thickness = 2 mm; Joshi et al. 2012), converted to voxel standardized uptake values based on body weight (SUVbw), and normalized into MNI space. Each scan was read by a fellowship-trained neuroradiologist blinded to group assignment and assessed as being "amyloid-positive" or "amyloid-negative" using established clinical criteria (Joshi et al. 2012). ADS patients who were amyloid-negative were excluded from the study.

MEG experimental paradigm and behavioral analysis

For MEG recording, participants were seated in a non-magnetic chair within a magnetically shielded room with their heads positioned within the sensor array, and completed a visuospatial discrimination task, termed "Vis-Attend" (Fig. 1a), to engage the visuospatial processing circuitry (Wiesman et al. 2017; Wiesman et al. 2018a; Wiesman and Wilson 2019). During this task, participants were told to fixate on a centrally presented crosshair. After a variable ISI (range: 1900–2100 ms), an 8 × 8 grid was presented for 800 ms at one of four locations relative to the fixation: above and to the right, below right, above left, or below left. The left and right orientations were defined as a lateral offset of 75% of the grid from the center of fixation. Participants were instructed to respond via button press with their right hand as to whether the grid was positioned to the left (index finger) or right (middle finger) of the fixation point upon presentation of the grid. Each participant performed 240 trials (60 of each type) in a pseudorandomized order concurrent with MEG recording. Responses with a reaction time 2.5 standard deviations (SDs) above or below the participant's mean were excluded prior to averaging. One-way ANCOVAs, controlling for the effect of age, were used to probe for group differences in reaction time and accuracy to ensure group differences in behavioral performance were not due to age discrepancies between groups. We first compared the behavioral metrics in healthy controls and patients (HAND + ADS) and then followed-up with participant group (ADS versus HAND) comparisons.

MEG data acquisition

MEG data acquisition, structural coregistration, preprocessing, and sensor-/source-level analyses followed a similar pipeline as a number of previous manuscripts from our laboratory (Spooner et al. 2019; Wiesman and Wilson 2020; Meehan et al. 2021). Briefly, all recordings took place in a one-layer magnetically shielded room with active shielding engaged for environmental noise compensation. A 306-sensor Elekta/MEGIN MEG system (Helsinki, Finland), equipped with 204 planar gradiometers and 102 magnetometers, was used to sample neuromagnetic responses continuously at 1 kHz with an acquisition bandwidth of 0.1–330 Hz. Participants were monitored by a real-time audio–video feed from inside the shielded room during MEG data acquisition. Each MEG dataset was individually corrected for head motion and subjected to noise reduction using the signal space separation method with a temporal extension

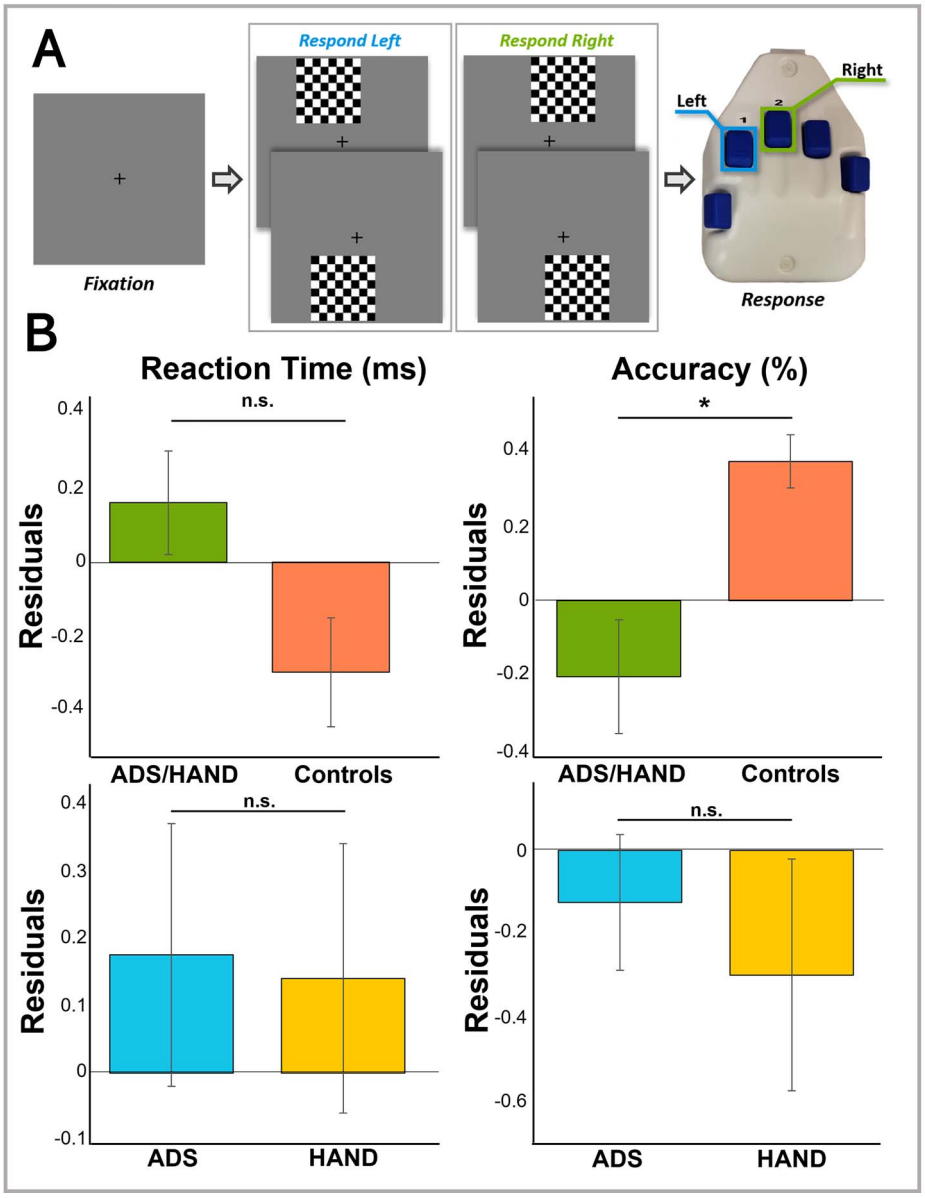

Fig. 1. Visuospatial processing task paradigm and behavioral outcomes. (a) A fixation crosshair was centrally presented for 2000 (±100) ms, followed by a checkerboard grid stimulus appearing in one of four locations (top left, bottom left, top right, bottom right) for 800 ms. Participants were instructed to respond via button press to indicate the laterality (left = right index finger, right = right middle finger) of the stimulus checkerboard relative to the fixation cross. (b) Residuals of reaction time and accuracy are given on the *y*-axis as a function of group accounting for the effect of age. Cognitively impaired participants (ADS/HAND patients) were less accurate than cognitively normal adults, but did not differ in reaction time. In general, patients on the ADS performed similar to patients with HAND. Error bars reflect the standard error of the mean (SEM). *$P < 0.05$.

(MaxFilter v2.2; correlation limit: 0.950; correlation window duration: 6 s; Taulu and Simola 2006). Only the gradiometer data was used in further analyses.

Structural MRI processing and MEG coregistration

Prior to MEG acquisition, four coils were attached to the participants' heads and localized, together with the three fiducial points and scalp surface, using a 3D digitizer (Fastrak 3SF0002, Polhemus Navigator Sciences, Colchester, VT, USA). Once positioned in the MEG, the coils produced an electrical current with a unique frequency label and an accompanying measurable magnetic field, which allowed each coil to be localized in reference to the MEG instrument sensors throughout recording. Since coil locations were also known in head coordinates, all MEG measurements could be transformed into a common coordinate system. With this coordinate system, each participant's MEG data were co-registered with structural T1-weighted MRI data using BESA MRI (Version 2.0) prior to source-space analysis. Structural MRI data were aligned parallel to the anterior and posterior commissures and transformed into standardized space.

MEG preprocessing, time–frequency transformation and sensor-level statistics

Cardiac and blink artifacts were identified in the raw MEG data and removed with signal-space projection

(SSP), which was subsequently accounted for during source reconstruction (Uusitalo and Ilmoniemi 1997). The continuous magnetic time series was then bandpass filtered between 0.5 and 200 Hz, plus a 60-Hz notch filter, and divided into 1500-ms epochs, with the baseline extending from −500 to 0 ms prior to the onset of the stimulus. Epochs containing artifacts were rejected using a fixed threshold method, supplemented with visual inspection. Briefly, in MEG, the raw signal amplitude is strongly affected by the distance between the brain and the MEG sensors, as the magnetic field strength falls off sharply as the distance from the current source increases. To account for this source of variance across participants, as well as other sources of variance, we used an individually determined threshold based on the within-subject signal distribution for both amplitude and gradient to reject artifacts. Across all participants, the average amplitude threshold for rejecting artifacts was 1093.75 (SD = 306.43) fT/cm and the average gradient threshold was 238.35 (SD = 127.36) fT/(cm × ms). Across all three groups, an average of 194.38 (SD = 26.12) out of 240 possible trials per participant were used for further analysis in this experiment. Importantly, our comparisons between groups were not affected by differences in the number of accepted trials per group, as this metric did not significantly differ across groups ($P = 0.25$).

Complex demodulation (Papp and Ktonas 1977; Kovach and Gander 2016) was used to transform the artifact-free epochs into the time–frequency domain, and the resulting spectral power estimations were averaged per sensor to generate time–frequency plots of mean spectral density. The time–frequency analysis was performed with a frequency step of 2 Hz and a time step of 25 ms between 4 and 100 Hz. These sensor-level data were then normalized by each respective bin's baseline power, calculated as the mean power during the −500 to 0 ms baseline period.

The specific time–frequency windows used for source imaging were determined by statistical analysis of the sensor-level spectrograms across all groups and the entire array of gradiometers. Each data point in each sensor-level spectrogram was initially evaluated using a mass univariate approach based on the general linear model. To reduce the risk of false positive results while maintaining reasonable sensitivity, a two-stage procedure was followed to control for Type 1 error. In the first stage, paired sample *t*-tests against baseline were conducted on each data point and the output spectrogram of *t*-values was thresholded at $P < 0.05$ to define time–frequency bins containing potentially significant oscillatory deviations across all participants. In stage two, the time–frequency bins that survived the threshold were clustered with temporally and/or spectrally neighboring bins (per sensor) that were also above the threshold ($P < 0.05$), and a cluster value was derived by summing all of the *t*-values of all data points in the cluster. Nonparametric permutation testing was then used to derive a distribution of cluster values and the significance level of the observed clusters (from stage one) were tested directly using this distribution (Ernst 2004; Maris and Oostenveld 2007). For each comparison, 10,000 permutations were computed to build a distribution of cluster values. Based on these analyses, significant time–frequency windows were identified and used to guide source-level analysis (all P's < 0.001). Cluster-based permutation testing on the MEG sensor-level data was performed in BESA Statistics (v2.1).

MEG source imaging

Cortical sources were imaged through an extension of the linearly constrained minimum variance vector beamformer (Van Veen et al. 1997; Gross et al. 2001; Hillebrand et al. 2005), which employs spatial filters in the frequency domain to calculate source power for the entire brain volume. The single images were derived from the cross spectral densities of all combinations of MEG gradiometers averaged over the time–frequency range of interest, and the solution of the forward problem for each location on a grid specified by input voxel space. In principle, the beamformer operator generates a spatial filter for each grid point that passes signals without attenuation from the given neural region, while suppressing activity in all other brain areas. The filter properties arise from the forward solution (lead field) for each location on a volumetric grid specified by input voxel space, and from the MEG covariance matrix. Basically, for each voxel, a set of beamformer weights is determined, which amounts to each MEG sensor being allocated a sensitivity weighting for activity in the particular voxel. This set of beamformer weights is the spatial filter unique to the given voxel, and this procedure is iterated until such a filter is computed for each voxel in the brain. Activity in each voxel is then determined independently and sequentially to produce a volumetric map of electrical activity with relatively high spatial resolution. In short, this method outputs a power value for each voxel in the brain, determined by a weighted combination of sensor-level time–frequency information. Following convention, the source power in these images was normalized per participant and image using a pre-stimulus noise period (i.e. baseline) of equal duration and bandwidth (Hillebrand et al. 2005). MEG preprocessing and imaging used the Brain Electrical Source Analysis (version 7.0) software.

Statistical analysis

Normalized source power was computed for the selected time frequency bands over the entire brain volume per participant at 4.0 × 4.0 × 4.0-mm resolution. Each participant's functional images were transformed into standardized space using the transform that was previously applied to the structural images and then spatially resampled. The resulting 3D maps of brain activity were averaged across all participants to qualitatively assess the anatomical basis of the significant

oscillatory responses identified through the sensor-level analysis. Using an ANCOVA approach with age as a nuisance covariate, our first-level analyses collapsed across patient groups (ADS + HAND) and aimed to identify regions where neural oscillatory responses differed between patients and controls. Brain regions where significant group differences were found were then probed to identify disease specific effects (i.e. ADS versus HAND). Bayes factors (BF_{01}) were also computed to evaluate the probability of the null for non-significant group comparisons between ADS and HAND. Our second-level analyses were more exploratory and compared the ADS and HAND groups directly at the whole-brain level for each oscillatory response. Our goals were to identify differences in regional processing between the two clinical groups. All statistical maps used an initial uncorrected significance threshold of $P < 0.001$ with a cluster threshold of $k = 5$. Whole-brain statistical computations and multiple comparisons correction were performed in SPM software version 12 (Wellcome Trust Centre for Neuroimaging). Finally, to assess neurobehavioral correlations, amplitude values were extracted from each significant peak per frequency band and related to task performance (e.g. reaction time and accuracy) and neuropsychological test scores using partial correlations that accounted for the effects of age.

Results

Behavioral analysis

Participants generally performed well on the task, as illustrated by considerably high accuracy ($M = 94.62\%$, $SD = 8.21\%$) and quick reaction time ($M = 610.15$ ms, $SD = 103.89$ ms). ANCOVAs accounting for the effect of age were used to assess group differences in performance on the visuospatial processing task (e.g. accuracy and reaction time; Fig. 1b). First, we collapsed across patient groups to examine behavioral performance in those with cognitive impairment compared to healthy controls. Our data indicated that patients were less accurate than controls ($F_{1,83} = 6.59$, $P = 0.012$) and that there were no differences in reaction time ($P = 0.09$). Next, we compared ADS and HAND groups and found that both groups performed similarly on the task in terms of accuracy ($P = 0.23$) and reaction time ($P = 0.86$).

MEG sensor-level analyses

In agreement with normative studies using this task (Wiesman et al. 2017; Wiesman et al. 2018a; Wiesman and Wilson 2019), sensor-level spectrograms revealed four significant clusters of task-relevant oscillatory activity (Fig. 2). Strong increases relative to baseline were identified in the theta band (4–8 Hz) from 0 to 250 ms (0 ms = stimulus onset) and the gamma range (40–58 Hz) from 350 to 600 ms (both $Ps < 0.001$, corrected). Significant decreases in alpha (8–14 Hz; 400–600 ms; $P < 0.001$, corrected) were also observed. Each of these neural responses were most robust in the gradiometers near posterior parietal and occipital cortices. Additionally, decreases in beta (16–22 Hz) oscillatory activity extended from 275 to 600 ms were detected in gradiometers near primary motor areas ($P < 0.001$, corrected). Of note, we limited the time windows used for imaging to 600 ms, as this was the average reaction time across all participants.

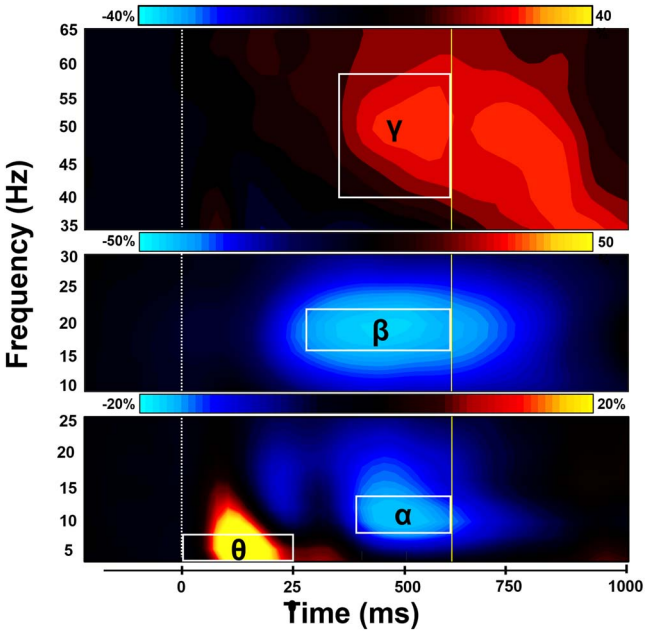

Fig. 2. Sensor-level time–frequency spectrograms. Time–frequency spectrograms showing task-related oscillatory responses averaged across trials and participants. Time is on the x-axis while frequency is displayed on the y-axis. Color bars above each spectrogram indicate the percent change in power from baseline. (Bottom) Strong increases in theta (4–8 Hz; 0–250 ms) and decreases in alpha activity (8–14 Hz; 400–600 ms) were observed in sensors near occipito-parietal cortices (MEG2522). (Middle) A robust decrease in beta power (16–22 Hz; 275–600 ms) over the sensorimotor cortices (MEG0222) was also observed. (Top) Increases in gamma (40–58 Hz) neural responses emerged 350–600 ms following stimulus onset in sensors near occipito-parietal areas (MEG2342). Each oscillatory response significantly differed from baseline ($P < 0.001$, corrected) and has been outlined and labeled accordingly. The dotted line (at 0 ms) indicates the stimulus onset, and the solid line (at 600 ms) represents average task reaction time.

MEG source-level analyses

To determine the neuroanatomical origins of the significant sensor-level oscillatory responses, each time–frequency window was imaged with a frequency-resolved beamformer. The images for each oscillatory response were then grand averaged across all participants (Fig. 3). The strongest increases in theta and gamma responses were generated by populations of neurons within the bilateral primary visual cortices, while the most robust alpha oscillations were distributed across the bilateral occipital and superior parietal cortices. Additionally, strong beta oscillatory responses were primarily clustered in the left primary motor cortex, and thus likely reflected the motor response. Consequently, we did not further probe the beta response as the goals of this study were to examine the oscillatory neural activity serving visuospatial processing.

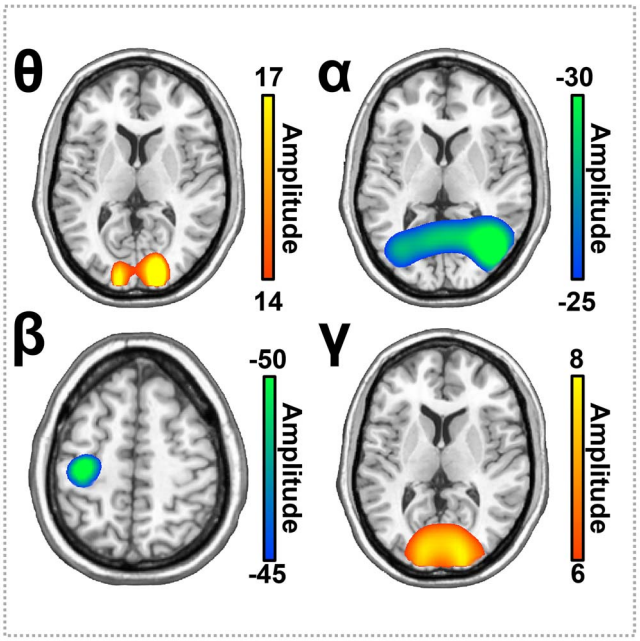

Fig. 3. Average whole-brain images of task-related neural oscillatory responses. Each image shows the grand average across all participants for each neural response. Neuronal populations in the bilateral primary visual cortices exhibited strong theta and gamma oscillations. In contrast, alpha oscillations were centered in more lateral occipital cortices bilaterally. Beta responses were centered in the contralateral primary motor cortex near the hand-knob feature. The color scale bar per image appears to the right in pseudo-t (amplitude) per voxel.

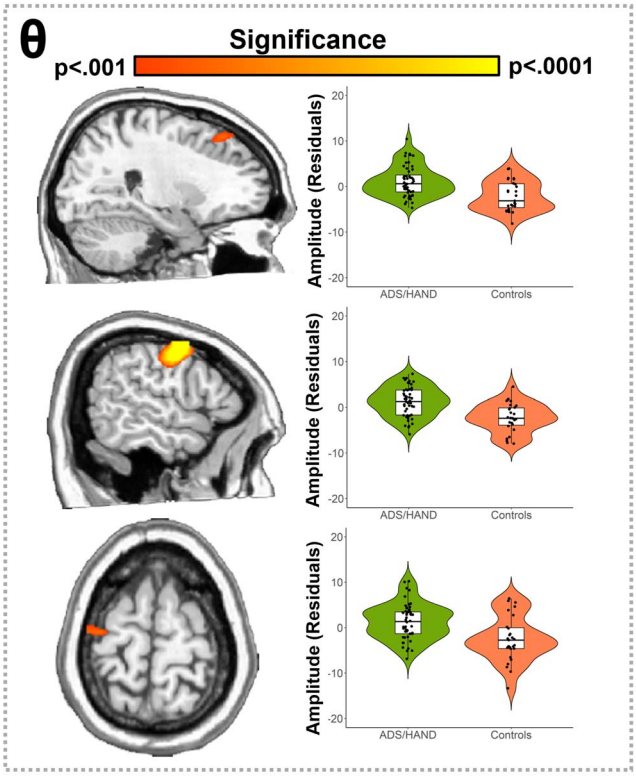

Fig. 4. Participants with ADS or HAND exhibited stronger theta responses during visuospatial processing than healthy controls. Whole-brain statistical maps assessing group differences in the theta band are shown on the left accompanied by violin plots for the peak voxel in each significant group difference cluster on the right. Group differences ($P < 0.001$, corrected) were found in the right dorsomedial prefrontal cortices (top), right dorsolateral prefrontal cortices (middle), and left precentral sulcus (bottom). Residuals of amplitude values controlling for age are presented in the right panel beside each corresponding brain slice.

Consistent with our behavioral analyses, we first collapsed across the ADS and HAND groups and performed ANCOVAs with age as a nuisance covariate to identify oscillatory differences between patients and controls. In the theta range, patients exhibited stronger responses compared to controls in the right dorsomedial prefrontal cortices, right dorsolateral prefrontal cortices, and left precentral sulcus (Fig. 4; $P < 0.001$, corrected). Post hoc testing of these responses indicated that the ADS and HAND groups each differed from controls, but did not differ from each other. This was largely confirmed by a follow-up Bayesian analysis that provided moderate evidence for the null hypothesis of no difference between ADS and HAND groups in the dorsomedial prefrontal cortex ($BF_{01} = 3.25$), dorsolateral prefrontal cortex ($BF_{01} = 3.53$), and precentral sulcus ($BF_{01} = 3.12$). Neurobehavioral correlation analyses indicated that theta oscillatory activity was not related to behavioral or neuropsychological metrics in these brain regions. No differences between patients (ADS + HAND) and controls were detected in the alpha or gamma range.

Finally, we conducted exploratory whole-brain analyses comparing ADS and HAND groups to identify any regional differences in neural processing. Our key findings indicated that those in the HAND group exhibited stronger alpha oscillations (i.e. more negative responses; $P < 0.001$, corrected; Fig. 5) compared to those on the ADS across multiple brain regions, including bilateral inferior parietal cortices (IPC), left medial prefrontal cortices, right inferior frontal gyrus (IFG), right superior temporal sulcus (STS), right middle temporal gyrus (MTG), and an area near the lateral geniculate nucleus. No significant group differences were found in the whole-brain comparisons of theta and gamma activity. Interestingly, we found a positive correlation between alpha activity in the left inferior parietal cortex and Hopkins Verbal Learning Test (HVLT) learning scores in participants with HAND ($r = 0.579$, $P = 0.009$), but no significant relationships in the ADS patients ($r = -0.263$, $P = 0.225$). This relationship between alpha activity in the left inferior parietal cortex and HVLT learning scores differed between groups ($Z = 2.77$, $P = 0.006$).

Discussion

While cognitive impairment in young PWH is commonly attributed to HAND, the origins of impairments emerging in PWH later in life, when susceptibility to age-related neurodegenerative diseases like AD increases, are potentially more complicated. However, our current understanding of the aberrant neural activity and cognitive features that distinguish ADS and HAND is extremely limited. In the current study, we examined the oscillatory

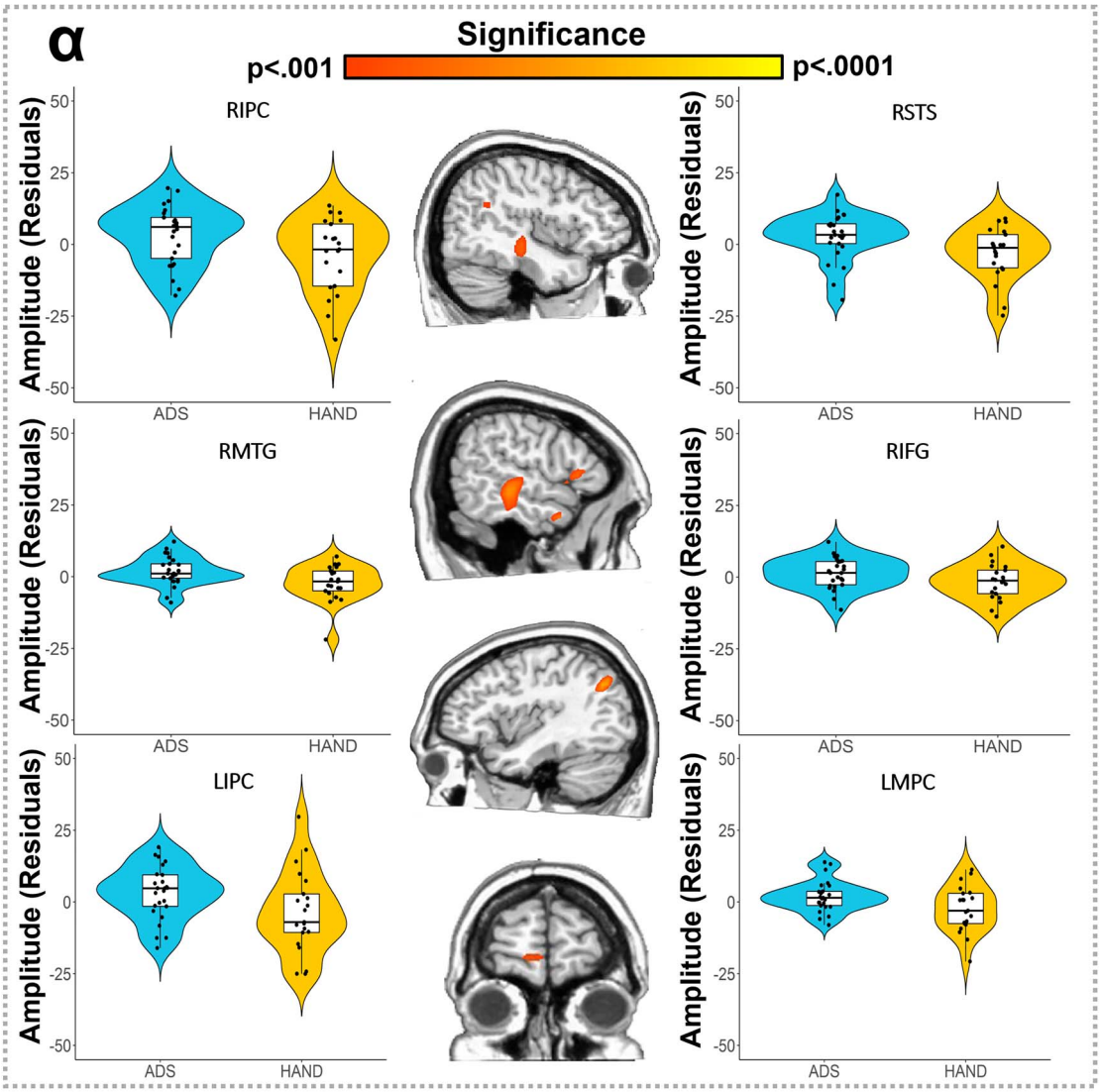

Fig. 5. Participants in the HAND group exhibited stronger alpha oscillations compared to those in the ADS group during visuospatial processing. Whole-brain group comparison maps for alpha activity are shown in the middle, with violin plots for the peak group difference voxel in each significant cluster shown in the flanking panels. Group differences ($P < 0.001$, corrected) were found in the bilateral IPC (top and bottom left), right STS (top right), right IFG (right middle), right MTG (left middle), and left medial prefrontal cortices (MPC; bottom right). Residuals of amplitude values controlling for age are presented on either side near the corresponding brain slices and labeled.

dynamics underlying visuospatial processing in persons with HAND, those on the ADS, and controls using MEG. Our findings revealed that both patient groups exhibited similar differences from controls in regards to reduced accuracy and stronger theta activity in prefrontal cortices. Conversely, our exploratory analyses indicated that alpha oscillatory activity across multiple brain regions distinguished the two clinical groups, with those with HAND exhibiting stronger alpha responses than those on the ADS. The implications of these findings are discussed in detail below.

Given the previous literature on visuospatial processing in healthy adults (Wiesman et al. 2017; Wiesman et al. 2018a; Wiesman and Wilson 2019), we expected task-related oscillations in the theta, alpha, and gamma range much like those observed. Previous work investigating visuospatial processing has also shown aberrations in theta oscillations in those with HAND, as well as abnormal spontaneous alpha and gamma cortical activity (Wiesman et al. 2018b). Studies focusing on adults with AD have shown that the strength of theta, alpha, and gamma oscillations during visuospatial processing is significantly predictive of group membership (i.e. patients versus controls; Wiesman et al. 2021b). Thus, we were not surprised by the robust theta, alpha, and gamma oscillations observed across the entire sample, nor the common differences between clinical patients (ADS + HAND) and controls in prefrontal theta oscillations. Essentially, patients in both groups exhibited stronger theta oscillations than controls in regions known to be critical for visual attention processing. Such increases in theta activity have been linked to the temporal segmentation and encoding of stimuli (Başar et al. 2001; Harris et al. 2017), and may reflect

compensatory processing in the current context, as the clinical groups performed similarly on the task. Additionally, this trend in behavior may indicate a speed-accuracy trade-off in the patient groups such that ADS and HAND patients sometimes responded before they were sure of the correct response (i.e. valued response time over accuracy), and this may be attributed to presence of cognitive impairment irrespective of pathology.

In addition to these nonspecific theta aberrations observed across both HAND and ADS groups, we found disease-specific markers in the alpha range across multiple brain regions in prefrontal, parietal, and temporal cortices. Alpha oscillations, especially in visual processing areas, are thought to be critical for the spatial disinhibition of neural populations involved in the processing visual information and enabling top–down control (Doesburg et al. 2016; van Diepen et al. 2016; Harris et al. 2017). Interestingly, aberrant alpha oscillatory dynamics are known to relate to cognitive status in patients with ADS and are known to be markers of cognitive impairment in PWH (Lew et al. 2018; Wiesman et al. 2018b; Wiesman et al. 2021b). Thus, the differences in neural dysfunction within the alpha frequency range in the context of visuospatial processing between ADS and HAND may be due to disease-specific alterations of the neurophysiological mechanisms coding for spatial or top-down cognitive properties of visual stimuli. Perhaps aberrant alpha activity in AD neuropathology is due to neurodegenerative elements of the disease, which along with tau accumulation, has been related to cognitive impairment (Bejanin et al. 2017; Huber et al. 2018; Malpetti et al. 2020). Regarding HAND, persistent neuroinflammation in PWH is thought to contribute to neurocognitive dysfunction and thus may be a key driver of the changes in alpha oscillations discussed herein (Hong and Banks 2015; Canet et al. 2018).

Importantly, these disease-specific aberrations in rhythmic alpha dynamics were found in key visuospatial processing regions. The most interesting regions differentially impacted by ADS and HAND were likely the bilateral inferior parietal cortices, left medial prefrontal cortices, and the right IFG. Aberrations in the left inferior parietal cortex were also differentially related to cognition by patient group, with alpha activity relating to learning in participants with HAND, but not in those on the ADS. This finding should be considered with caution as a sizable portion of learning scores were very low and near or at floor levels in participants with ADS. Moreover, these fronto-parietal regions are known to contribute to visuospatial processing and the deployment of attention (Corbetta and Shulman 2002; Fan et al. 2005; Wu et al. 2016), and work has also linked these regions, especially the right inferior frontal cortices to top-down mechanisms modulating visuospatial perception and subsequent processing (Daffner et al. 2000; Corbetta and Shulman 2002; Fan et al. 2005). Thus, disease-specific disruption of alpha oscillations in these areas was not surprising, as previous studies in AD and HAND independently have reported aberrations in visuospatial processing-related alpha activity (Chang et al. 2001; Prvulovic et al. 2002; Chang et al. 2004; Thiyagesh et al. 2009; Lew et al. 2018; Wiesman et al. 2021b), although the observation that these altered dynamics are disease specific is especially intriguing and future studies should probe whether these differences are related to clinical metrics such as disease severity, duration, and other factors. Furthermore, it should be noted that the past studies reporting differences between controls and those with HAND or AD focused on the neural dynamics within occipital cortices, while the current study took a whole-brain approach. Thus, our lack of occipital findings do not refute the prior work and our findings of prefrontal differences are not in direct conflict. The same caveats apply to the spectral differences we observed.

Beyond frontoparietal cortices, we also found disease-specific differences in temporal regions. Previous research has found that alpha oscillatory activity in temporal cortices promotes top-down control (Doesburg et al. 2016), which may extend to cognitive control of visuospatial processing and attention. Visuospatial functions have been found to be affected by tau pathology in occiptotemporal regions in AD (Prvulovic et al. 2002; Bejanin et al. 2017), and atypical activation and degradation of the temporal lobes have been reported in PWH (Woods et al. 2013; Israel et al. 2019). The particular region of the right STS where group differences were found has been associated with polysensory integration of stimuli and the organization of visuospatial stimuli for hierarchical visual processing (Falchier et al. 2002; Beauchamp 2005; Barton and Brewer 2017). Therefore, abnormal activity in these cortical areas may suggest ineffective organization and integration of sensory information at early stages of visual processing and may have downstream effects in higher order visuospatial areas. Our finding of group differences in the LGN may reflect even earlier deficits along thalamocortical visual pathways, although caution is warranted given the depth of this response and the limited sensitivity of MEG to sources far away from the sensors (Hillebrand and Barnes 2002).

Together, the findings of this study provide a foundation for understanding the neurophysiological mechanisms underlying cognitive impairment in HAND and ADS. Despite the importance of these outcomes, this study is not without limitations. First, though all ADS participants were biomarker confirmed using amyloid PET, we did not have data on amyloid deposition of all controls and those with HAND. Future studies examining ADS and HAND in conjunction should include PET imaging on all participants and attempt to link amyloid deposition to MEG markers of each condition. A second limitation of the current study was related to task simplicity, which may explain the absence of reaction time differences between patients with HAND and those on the ADS.

While both ADS and HAND patients typically exhibit deficits in visuospatial processing, assessing more complex cognitive functions may also be a promising future direction. Patients diagnosed with ADS and HAND generally exhibit cognitive and neural dysfunction in working memory, attention, and other processes (Chang et al. 2001; Antinori et al. 2007; Milanini and Valcour 2017; Milanini et al. 2019) and each diagnosis is known to have aberrations in rhythmic neural activity associated with these processes (e.g. theta, alpha, and gamma oscillations; (Wilson et al. 2013; Lew et al. 2018; Groff et al. 2020; Wiesman et al. 2021a, 2021b). Considering this study found disease-specific alpha aberrations underlying visuospatial processing, examining other cognitive processes that are known to be served by regional alpha oscillations may be of particular interest (e.g. attention and working memory).

Conclusion

To close, we found aberrant prefrontal theta oscillations that were common across both HAND and ADS diagnoses relative to controls, along with disease-specific deficits in the alpha range across a network of brain regions serving visuospatial processing. Weaker alpha responses in patients on the ADS compared to those with HAND may suggest distinguishable neurophysiological features of visuospatial dysfunction. This study is the first to examine dynamic oscillatory differences among patients on the ADS and those with HAND during visuospatial processing, and provides critical data suggesting both disease-common and disease-specific oscillatory signatures may reflect features of the neuropathology underlying each condition.

Acknowledgments

We would like to thank the participants for volunteering to participate in the study, as well as our staff and local collaborators for their contributions to the work. We would also like to specifically thank Nichole Knott and Katie Losh for assistance with the MEG recordings.

Supplementary material

Supplementary material is available at *Cerebral Cortex* online.

Funding

This research was supported by grants R01-MH116782 (TWW), R01-MH118013 (TWW), P20-GM144641 (TWW), F31-AG055332 (AIW), F32-NS119375 (AIW), and F31-DA056296 (MS) from the National Institutes of Health. The funders had no role in study design, data collection and analysis, decision to publish, or preparation of the manuscript.

Conflict of interest statement: None declared.

References

Antinori A, Arendt G, Becker JT, Brew BJ, Byrd DA, Cherner M, Clifford DB, Cinque P, Epstein LG, Goodkin K, et al. Updated research nosology for HIV-associated neurocognitive disorders. *Neurology*. 2007:69:1789–1799.

Aylward EH, Brettschneider PD, McArthur JC, Harris GJ, Schlaepfer TE, Henderer JD, Barta PE, Tien AY, Pearlson GD. Magnetic resonance imaging measurement of gray matter volume reductions in HIV dementia. *Am J Psychiatry*. 1995:152:987–994.

Barton B, Brewer AA. Visual field map clusters in high-order visual processing: organization of V3A/V3B and a new cloverleaf cluster in the posterior superior temporal sulcus. *Front Integr Neurosci*. 2017:11:4.

Başar E, Başar-Eroglu C, Karakaş S, Schürmann M. Gamma, alpha, delta, and theta oscillations govern cognitive processes. *Int J Psychophysiol*. 2001:39:241–248.

Beauchamp MS. See me, hear me, touch me: multisensory integration in lateral occipital-temporal cortex. *Curr Opin Neurobiol*. 2005:15:145–153.

Bejanin A, Schonhaut DR, La Joie R, Kramer JH, Baker SL, Sosa N, Ayakta N, Cantwell A, Janabi M, Lauriola M, et al. Tau pathology and neurodegeneration contribute to cognitive impairment in Alzheimer's disease. *Brain J Neurol*. 2017:140:3286–3300.

Benedict RHB, Schretlen D, Groninger L, Brandt J. Hopkins verbal learning test – revised: normative data and analysis of inter-form and test-retest reliability. *Clin Neuropsychol*. 1998:12(1):43–55.

Brandt J, Benedict RHB. *Hopkins verbal learning test – revised: professional manual*. Lutz, FL: Psychological Assessment Resources; 2001

Buzsáki G, Wang X-J. Mechanisms of gamma oscillations. *Annu Rev Neurosci*. 2012:35:203–225.

Calcagno A, Celani L, Trunfio M, Orofino G, Imperiale D, Atzori C, Arena V, d'Ettorre G, Guaraldi G, Gisslen M, et al. Alzheimer dementia in people living with HIV. *Neurol Clin Pract*. 2021:11:e627–e633.

Canet G, Dias C, Gabelle A, Simonin Y, Gosselet F, Marchi N, Makinson A, Tuaillon E, Van de Perre P, Givalois L, et al. HIV neuroinfection and Alzheimer's disease: similarities and potential links? *Front Cell Neurosci*. 2018:12:1–12.

Chang L, Speck O, Miller EN, Braun J, Jovicich J, Koch C, Itti L, Ernst T. Neural correlates of attention and working memory deficits in HIV patients. *Neurology*. 2001:57:1001–1007.

Chang L, Tomasi D, Yakupov R, Lozar C, Arnold S, Caparelli E, Ernst T. Adaptation of the attention network in human immunodeficiency virus brain injury. *Ann Neurol*. 2004:56:259–272.

Corbetta M, Shulman GL. Control of goal-directed and stimulus-driven attention in the brain. *Nat Rev Neurosci*. 2002:3:201–215.

Daffner KR, Mesulam MM, Scinto LFM, Acar D, Calvo V, Faust R, Chabrerie A, Kennedy B, Holcomb P. The central role of the prefrontal cortex in directing attention to novel events. *Brain*. 2000:123:927–939.

Doesburg SM, Bedo N, Ward LM. Top-down alpha oscillatory network interactions during visuospatial attention orienting. *NeuroImage*. 2016:132:512–519.

Ernst MD. Permutation methods: a basis for exact inference. *Stat Sci*. 2004:19:676–685.

Falchier A, Clavagnier S, Barone P, Kennedy H. Anatomical evidence of multimodal integration in primate striate cortex. *J Neurosci*. 2002:22:5749–5759.

Fan J, McCandliss BD, Fossella J, Flombaum JI, Posner MI. The activation of attentional networks. *NeuroImage*. 2005:26:471–479.

Folstein MF, Folstein SE, McHugh PR. "Mini-mental state". A practical method for grading the cognitive state of patients for the clinician. *J Psychiatr Res*. 1975:12:189–198.

Fulop T, Witkowski JM, Larbi A, Khalil A, Herbein G, Frost EH. Does HIV infection contribute to increased beta-amyloid synthesis and plaque formation leading to neurodegeneration and Alzheimer's disease? *J Neuro-Oncol*. 2019:25:634–647.

Groff BR, Wiesman AI, Rezich MT, O'Neill J, Robertson KR, Fox HS, Swindells S, Wilson TW. Age-related visual dynamics in HIV-infected adults with cognitive impairment. *Neurol: Neuroimmunol Neuroinflammation*. 2020:7:1–12.

Gross J, Kujala J, Hämäläinen M, Timmermann L, Schnitzler A, Salmelin R. Dynamic imaging of coherent sources: studying neural interactions in the human brain. *Proc Natl Acad Sci*. 2001:98: 694–699.

Harris AM, Dux PE, Jones CN, Mattingley JB. Distinct roles of theta and alpha oscillations in the involuntary capture of goal-directed attention. *NeuroImage*. 2017:152:171–183.

Heaton RK, Miller SW, Taylor MJ, Grant I. *Revised comprehensive norms for an expanded Halstead-Reitan battery: demographically adjusted neuropsychological norms for African American and Caucasian adults*. Lutz, FL: Psychological Assessment Resources; 2004.

Hillebrand A, Barnes GR. A quantitative assessment of the sensitivity of whole-head MEG to activity in the adult human cortex. *NeuroImage*. 2002:16:638–650.

Hillebrand A, Singh KD, Holliday IE, Furlong PL, Barnes GR. A new approach to neuroimaging with magnetoencephalography. *Hum Brain Mapp*. 2005:25:199–211.

Hong S, Banks WA. Role of the immune system in HIV-associated neuroinflammation and neurocognitive implications. *Brain Behav Immun*. 2015:45:1–12.

Howdle GC, Quidé Y, Kassem MS, Johnson K, Rae CD, Brew BJ, Cysique LA. Brain amyloid in virally suppressed HIV-associated neurocognitive disorder. *Neurol: Neuroimmunol Neuroinflammation*. 2020:7:1–11.

Huber CM, Yee C, May T, Dhanala A, Mitchell CS. Cognitive decline in preclinical Alzheimer's disease: amyloid-Beta versus Tauopathy. *J Alzheimer's Dis*. 2018:61:265–281.

Israel SM, Hassanzadeh-Behbahani S, Turkeltaub PE, Moore DJ, Ellis RJ, Jiang X. Different roles of frontal versus striatal atrophy in HIV-associated neurocognitive disorders. *Hum Brain Mapp*. 2019:40: 3010–3026.

Joshi AD, Pontecorvo MJ, Clark CM, Carpenter AP, Jennings DL, Sadowsky CH, Adler LP, Kovnat KD, Seibyl JP, Arora A, et al. Performance characteristics of amyloid PET with Florbetapir F 18 in patients with Alzheimer's disease and cognitively normal subjects. *J Nucl Med*. 2012:53:378–384.

Kovach CK, Gander PE. The demodulated band transform. *J Neurosci Methods*. 2016:261:135–154.

Lane CA, Hardy J, Schott JM. Alzheimer's disease. *Eur J Neurol*. 2018:25: 59–70.

Lew BJ, McDermott TJ, Wiesman AI, O'Neill J, Mills MS, Robertson KR, Fox HS, Swindells S, Wilson TW. Neural dynamics of selective attention deficits in HIV-associated neurocognitive disorder. *Neurology*. 2018:91:e1860–e1869.

Malpetti M, Kievit RA, Passamonti L, Jones PS, Tsvetanov KA, Rittman T, Mak E, Nicastro N, Bevan-Jones WR, Su L, et al. Microglial activation and tau burden predict cognitive decline in Alzheimer's disease. *Brain J Neurol*. 2020:143:1588–1602.

Maris E, Oostenveld R. Nonparametric statistical testing of EEG- and MEG-data. *J Neurosci Methods*. 2007:164:177–190.

Meehan CE, Wiesman AI, Spooner RK, Schantell M, Eastman JA, Wilson TW. Differences in rhythmic neural activity supporting the temporal and spatial cueing of attention. *Cereb Cortex*. 2021:31: 4933–4944.

Milanini B, Valcour V. Differentiating HIV-associated neurocognitive disorders from Alzheimer's disease: an emerging issue in geriatric neuro HIV. *Curr HIV/AIDS Rep*. 2017:14: 123–132.

Milanini B, Samboju V, Cobigo Y, Paul R, Javandel S, Hellmuth J, Allen I, Miller B, Valcour V. Longitudinal brain atrophy patterns and neuropsychological performance in older adults with HIV-associated neurocognitive disorder compared with early Alzheimer's disease. *Neurobiol Aging*. 2019:82:69–76s.

Minoshima S, Drzezga AE, Barthel H, Bohnen N, Djekidel M, Lewis DH, Mathis CA, McConathy J, Nordberg A, Sabri O, et al. SNMMI procedure standard/EANM practice guideline for amyloid PET imaging of the brain 1.0. *J Nucl Med*. 2016:57:1316–1322.

Mohamed M, Skolasky RL, Zhou Y, Ye W, Brasic JR, Brown A, Pardo CA, Barker PB, Wong DF, Sacktor N. Beta-amyloid (Aβ) uptake by PET imaging in older HIV+ and HIV- individuals. *J Neuro-Oncol*. 2020:26:382–390.

Namagga JK, Rukundo GZ, Voss JG. Prevalence and risk factors of HIV-associated neurocognitive disorders in rural Southwestern Uganda. *J Assoc Nurses AIDS Care*. 2019:30:531–538.

Nasreddine ZS, Phillips NA, Bédirian V, Charbonneau S, Whitehead V, Collin I, Cummings JL, Chertkow H. The Montreal Cognitive Assessment, MoCA: a brief screening tool for mild cognitive impairment. *J Am Geriatr Soc*. 2005:53:695–699.

Papp N, Ktonas P. Critical evaluation of complex demodulation techniques for the quantification of bioelectrical activity. *Biomed Sci Instrum*. 1977:13:135–145.

Pfeffer RI, Kurosaki TT, Harrah CH, Chance JM, Filos S. Measurement of functional activities in older adults in the community. *J Gerontol*. 1982:37:323–329.

Prvulovic D, Hubl D, Sack AT, Melillo L, Maurer K, Frölich L, Lanfermann H, Zanella FE, Goebel R, Linden DEJ, et al. Functional imaging of visuospatial processing in Alzheimer's disease. *NeuroImage*. 2002:17:1403–1414.

Robertson KR, Smurzynski M, Parsons TD, Wu K, Bosch RJ, Wu J, McArthur JC, Collier AC, Evans SR, Ellis RJ. The prevalence and incidence of neurocognitive impairment in the HAART era. *Aids*. 2007:21:1915–1921.

Rubin LH, Sundermann EE, Moore DJ. The current understanding of overlap between characteristics of HIV-associated neurocognitive disorders and Alzheimer's disease. *J Neuro-Oncol*. 2019:25:661–672.

Spooner RK, Wiesman AI, Proskovec AL, Heinrichs-Graham E, Wilson TW. Rhythmic spontaneous activity mediates the age-related decline in somatosensory function. *Cereb Cortex*. 2019:29:680–688.

Taulu S, Simola J. Spatiotemporal signal space separation method for rejecting nearby interference in MEG measurements. *Phys Med Biol*. 2006:51:1759–1768.

Thiyagesh SN, Farrow TFD, Parks RW, Accosta-Mesa H, Young C, Wilkinson ID, Hunter MD, Woodruff PWR. The neural basis of visuospatial perception in Alzheimer's disease and healthy elderly comparison subjects: an fMRI study. *Psychiatry Res Neuroimaging*. 2009:172:109–116.

Turner RS, Chadwick M, Horton WA, Simon GL, Jiang X, Esposito G. An individual with human immunodeficiency virus, dementia, and central nervous system amyloid deposition. *Alzheimer's Dement: Diagn Assess Dis Monit*. 2016:4:1–5.

Uusitalo MA, Ilmoniemi RJ. Signal-space projection method for separating MEG or EEG into components. *Med Biol Eng Comput*. 1997:35: 135–140.

van Diepen RM, Miller LM, Mazaheri A, Geng JJ. The role of alpha activity in spatial and feature-based attention. *eNeuro*. 2016:3: 1–11.

Van Veen BD, Van Drongelen W, Yuchtman M, Suzuki A. Localization of brain electrical activity via linearly constrained minimum variance spatial filtering. *IEEE Trans Biomed Eng*. 1997:44: 867–880.

Vannini P, Lehmann C, Dierks T, Jann K, Viitanen M, Wahlund L-O, Almkvist O. Failure to modulate neural response to increased task demand in mild Alzheimer's disease: fMRI study of visuospatial processing. *Neurobiol Dis*. 2008:31:287–297.

Wiesman AI, Wilson TW. The impact of age and sex on the oscillatory dynamics of visuospatial processing. *NeuroImage*. 2019:185: 513–520.

Wiesman AI, Wilson TW. Attention modulates the gating of primary somatosensory oscillations. *NeuroImage*. 2020:211:116610.

Wiesman AI, Heinrichs-Graham E, Proskovec AL, McDermott TJ, Wilson TW. Oscillations during observations: dynamic oscillatory networks serving visuospatial attention. *Hum Brain Mapp*. 2017:38: 5128–5140.

Wiesman AI, Mills MS, McDermott TJ, Spooner RK, Coolidge NM, Wilson TW. Polarity-dependent modulation of multi-spectral neuronal activity by transcranial direct current stimulation. *Cortex*. 2018a:108:222–233.

Wiesman AI, O'Neill J, Mills MS, Robertson KR, Fox HS, Swindells S, Wilson TW. Aberrant occipital dynamics differentiate HIV-infected patients with and without cognitive impairment. *Brain*. 2018b:141:1678–1690.

Wiesman AI, Murman DL, May PE, Schantell M, Losh RA, Johnson HJ, Willet MP, Eastman JA, Christopher-Hayes NJ, Knott NL, et al. Spatio-spectral relationships between pathological neural dynamics and cognitive impairment along the Alzheimer's disease spectrum. *Alzheimer's Dement*. 2021a:13:e12200.

Wiesman AI, Murman DL, May PE, Schantell M, Wolfson SL, Johnson CM, Wilson TW. Visuospatial alpha and gamma oscillations scale with the severity of cognitive dysfunction in patients on the Alzheimer's disease spectrum. *Alzheimers Res Ther*. 2021b: 13:139.

Wilson TW, Heinrichs-Graham E, Robertson KR, Sandkovsky U, O'Neill J, Knott NL, Fox HS, Swindells S. Functional brain abnormalities during finger-tapping in HIV-infected older adults: a magnetoencephalography study. *J Neuroimmune Pharmacol*. 2013:8964–974. https://doi.org/10.1007/s11481-013-9477-1.

Woods SP, Moore DJ, Weber E, Grant I. Cognitive neuropsychology of HIV-associated neurocognitive disorders. *Neuropsychol Rev*. 2009:19:152–168.

Woods SP, Hoebel C, Pirogovsky E, Rooney A, Cameron MV, Grant I, Gilbert PE. Visuospatial temporal order memory deficits in older adults with HIV infection. *Cogn Behav Neurol*. 2013:26:171–180.

Wu Y, Wang J, Zhang Y, Zheng D, Zhang J, Rong M, Wu H, Wang Y, Zhou K, Jiang T. The neuroanatomical basis for posterior superior parietal lobule control lateralization of visuospatial attention. *Front Neuroanat*. 2016:10:1–9.